Int J Adv Manuf Technol (2017) 90:2163–2172
DOI 10.1007/s00170-016-9494-3

ORIGINAL ARTICLE

Non-contact on-machine measurement using a chromatic confocal probe for an ultra-precision turning machine

Xicong Zou[1] · **Xuesen Zhao**[1] · **Guo Li**[2] · **Zengqiang Li**[1] · **Tao Sun**[1]

Received: 18 June 2016 / Accepted: 16 September 2016 / Published online: 10 October 2016

Abstract On-machine measurement (OMM) involves the interruption of the machining process and the subsequent measurement of the workpiece without its removal from the machining tool. Chromatic confocal sensing is a well-known measurement technique that is able to evaluate the position of a point on an object surface along the optical axis of the system with high accuracy. The present study integrates a chromatic confocal measurement probe with an ultra-precision diamond turning machine to achieve the non-contact OMM of machined components. The procedure for establishing the position of the rotary axis of the spindle based on dual standard spheres is first described in detail, and the relevant OMM procedure for machined components of different surface topographies is explained. Then, a 50-μm quartz step height standard is employed to investigate the linear measurement accuracy of the chromatic confocal probe. Finally, the measurement accuracy of the proposed OMM method is compared experimentally with that of the stylus method. The results show that the estimated form error value of the OMM method agrees well with the value obtained by the stylus method. The proposed OMM method feasibly achieves non-contact OMM with a nanometer-level accuracy for an ultra-precision turning machine and is capable of reconstructing the 3D surface topography of flat, spherical, and aspheric surfaces. After integrating the OMM method, the ultra-precision turning machine can realize the function of processing-measurement integration.

Keywords On-machine measurement · Non-contact · Chromatic confocal probe · Dual-sphere calibration · 3D surface topography

Electronic supplementary material The online version of this article (doi:10.1007/s00170-016-9494-3) contains supplementary material, which is available to authorized users.

✉ Xuesen Zhao
zxs0327@126.com

[1] Center of Precision Engineering, Harbin Institute of Technology, Harbin 150001, People's Republic of China

[2] Research Center of Laser Fusion, China Academy of Engineering Physics, Mianyang 621900, People's Republic of China

1 Introduction

The validation of a machining process often requires conducting machining accuracy measurements. However, the use of 3D measurement instruments typically requires the removal of the workpiece from the machine tool, which can introduce systematic errors. On-machine measurement (OMM) can overcome this disadvantage. OMM is a type of in-process measurement or post-process measurement, also denoted as an in situ or process-intermittent measurement method, that involves the interruption of the machining process, and the subsequent measurement of the workpiece without its removal from the machining tool [1, 2]. OMM has shown remarkable achievements regarding high precision and rapid measurement, and OMM applications have been extensively developed over the past several decades. Shiraishi [3] summarized the development of in-process measurement and OMM methods from 1961 to 1985. Yandayan and Burdekin [4] presented an investigation of existing methods from 1986 to 1996. Vacharanukul and Mekid [1] extended the survey of papers proposing in-process measurement and OMM methods up to 2003. OMM techniques can be categorized according to the type of sensor employed as probe contact methods [5–9] and optical non-contact methods [10–19]. Probe contact methods employ a stylus or probe in

contact with the surface of a machined component to achieve a section profile. As such, the probe will affect the smoothness of the workpiece surface to some degree, which induces measurement error [20]. All non-contact OMM methods are non-destructive and share the common advantages of high efficiency and high accuracy. Chromatic confocal sensing is a well-known measurement technique that is able to evaluate the position of a point on an object surface along the optical axis of the system with high accuracy and has attracted considerable attention. Luo et al. [21] proposed a chromatic confocal system based on a large-diameter optical fiber that provided for a very high detection efficiency. In this system, the Gaussian mixture model was considered best relative to three other data processing methods, and the system was sufficiently stable and accurate with a long-term standard deviation of 0.16 mm and a short-term deviation of 0.07 mm. Quinsat and Tournier [22] presented an OMM method to measure the surface topography of a machined component. The thermal effects and z-axis repeatability of the machining tool were taken into consideration, and compensation for thermal effects on the measurement results was discussed. The finishing process was assessed by applying the method to a five-axis machining center. Minoni et al. [23] proposed a new OMM method employing a chromatic confocal probe, a super continuum light source, and a spatial filter. The spectra were normalized and fitted to Gaussian forms prior to extracting the displacement information, and experimental results demonstrated that the proposed method improved measurement accuracy by nearly one order of magnitude relative to other existing supercontinuum-based confocal systems. Nouira et al. [24] integrated two chromatic confocal probes into a high-precision profilometer and designed a new calibration bench for characterizing the main sources of measurement error for the chromatic confocal probe. The displacement measurements obtained from the two chromatic confocal probes were compared with that obtained from a laser interferometer serving as a reference to ensure measurement traceability. The main sources of error, such as the material characteristics, surface reflectivity, scanning speed, and surface roughness, were successfully identified, and the experimental results showed that chromatic confocal probe measurements were sensitive to these errors. Rishikesan and Samuel [25] employed a chromatic confocal displacement sensor to estimate the surface profile parameters of different machined surfaces, and the surface parameters obtained agreed well with the results of the stylus method.

The literature review presented indicates that a great deal of work has been conducted for characterizing the error sources, improving the accuracy, and optimizing the performance of chromatic confocal probes. However, relatively few investigations have been conducted for the reconstruction of 3D surface, alignment of the relative distance between the c-axis and measurement probe, and processing-measurement integration in a three-axis ultra-precision machining tool. Thus, to rectify the deficiency, the present work studies this specific application in a manner that proceeds from a theoretical foundation toward the practical application.

In the present study, a chromatic confocal measurement probe is integrated into an ultra-precision diamond turning machine to achieve the non-contact OMM of the machined surface. A vertical high-precision translation stage (M-505.2DG from Physik Instrumente, Karlsruhe, Germany), which moves along the y direction, is employed to control the position of the measurement probe. The x and z slideways of the turning machine, driven by linear motors, control the relative position between the measured workpiece and measurement probe in the x and z directions. The basis of the OMM method is clearly described, and the working principles of a chromatic confocal sensor and the data acquisition system are introduced. Measurement accuracy and the evaluation of uncertainty are discussed in detail. To validate the effectiveness of the proposed OMM system, a series of cutting experiments are conducted on the ultra-precision diamond turning machine, and the measurement accuracy of the proposed OMM system is compared with that of the Talysurf PGI 1240 (Taylor Hobson Ltd., Leicester, UK) dedicated contact-type metrology instrument, which is employed as a reference device.

The remainder of this paper is organized as follows. First, the sensor parameters and the measurement procedure are presented, and the experimental details are described in Sect. 2. The measurement accuracy and uncertainty analysis are discussed in detail, and the experimental measurement comparison is discussed in Sect. 3. Finally, Sect. 4 provides concluding remarks.

2 Methodology

2.1 System configuration

The proposed OMM system is shown in Fig. 1. The system is composed of an aerostatic spindle and vacuum chuck, two horizontal hydrostatic slideways (x- and z-axes), an orthogonal y-axis precision stage, a chromatic confocal probe mounted on the y-axis translation stage, a standard 12.7-mm radius sphere affixed in the vacuum chuck (the master sphere), and a second standard 6.2-mm radius sphere (the reference sphere) mounted to a granite base located on top of the spindle via a dedicated transition arm attached to a standard System 3R holder (GF Machining Solutions). As such, the chromatic confocal probe and the y-axis translation stage form an integrated component of the OMM system and the reference sphere and transition arm form another integrated component. The y-axis precision stage is bolted onto the z-directional slideway. The optical axis of the measurement probe is

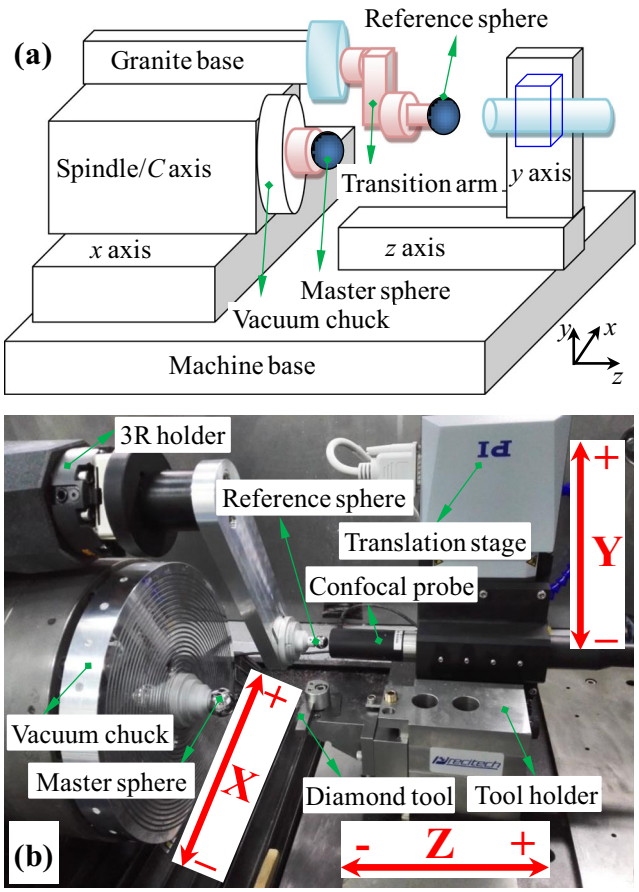

Fig. 1 The proposed on-machine measurement (OMM) system: **a** schematic diagram of the OMM system; **b** image of the OMM system

adjusted to be collinear to the z direction, although a perfect collinear relationship is not required. The spindle and vacuum chuck are positioned on the x-directional slideway. The standard spheres must be of sufficiently high geometric accuracy and are employed to calibrate the relative distance between the rotary axis of the spindle and the center of the reference sphere, which is further discussed in Sect. 2.2.

The CL1 MG140 non-contact point sensor (STIL, France) was employed to evaluate the surface topography based on chromatic confocal sensing technology. The chromatic confocal probe is connected to its dedicated controller (CCS-Prima from STIL, France) through an optical fiber, and the controller is connected to a UMac data acquisition card for data acquisition and storage.

The optical principles of a chromatic confocal probe are illustrated in Fig. 2. The white light point source passes through an objective lens, which diffracts the emerging light according to its wavelength. Only light of a wavelength λM is focused at a point M on the surface being measured. The backscattered light passes back through the objective lens and is then directed toward the detector by a beamsplitter. The pinhole located at the image of M plays an essential role in this system because it filters

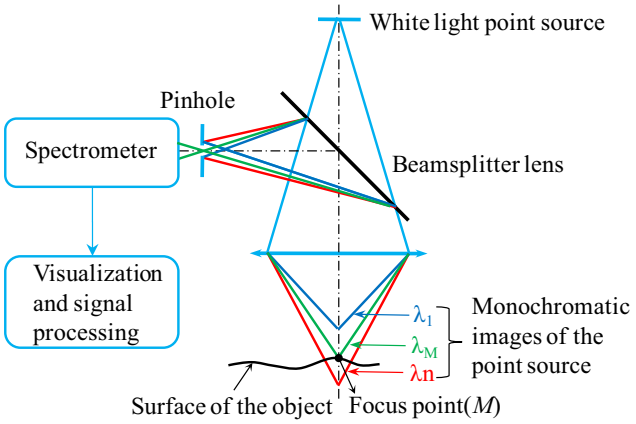

Fig. 2 The optical principles of a chromatic confocal probe

out all wavelengths except λM that derive from points located on the optical axis above or below M.

The linear displacement accuracy of the chromatic confocal probe employed in the present study was investigated by means of a 50-μm quartz step height standard (SHS-50.0QC, serial number 7657-73-12, VLSI Standards, Inc.) that was calibrated by the National Institute of Standards and Technology (NIST), yielding a height of 49.6709 μm with an uncertainty of 0.11488 μm. The standard step was sucked in the vacuum chuck by vacant absorption force. The measurement probe was mounted to the y-axis precision stage, and the optical axis of the measurement probe is perpendicular to the surface of standard step. A linear scanning measurement (the linear movement of the standard step along the x direction) was performed on the standard step, and the measurement result is shown in Fig. 3. Based on the respective minimum and maximum heights of −8.64 and 41.02 in the y direction, the measured height is 49.66 μm, yielding a deviation of 0.011 μm from the actual standard step height. The relative measurement error (RME) can be calculated as

$$RME = \frac{|49.66-49.6709|}{49.6709} \times 100\% = 0.022\%. \quad (1)$$

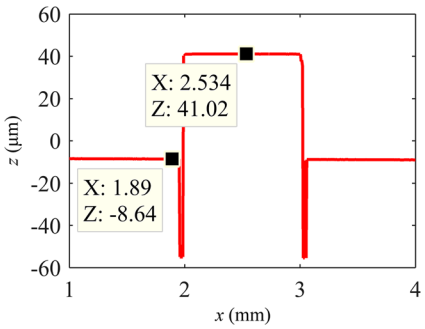

Fig. 3 The height measurement result of a 50-μm quartz height step standard

The *RME* is relatively small, indicating that the measurement probe provides excellent linear measurement accuracy and is therefore ideally suited for OMM.

2.2 Calibration based on dual standard spheres

Before conducting measurements, it is first necessary to calibrate the relative distance between the rotary axis of the spindle (henceforth denoted as the *c*-axis) and the center of the reference sphere. Initially, the master sphere is installed in the vacuum chuck and the eccentric error between the center of the master sphere and the *c*-axis is measured by an inductance micrometer. This error can be reduced to less than 0.1 μm by manually adjusting the location of the master sphere. The detailed calibration procedure is described as follows.

1. The first stage involves aligning the chromatic confocal probe with the *c*-axis, which, in effect, involves aligning the probe with the center position coordinate of the master sphere. The calibration procedure is illustrated in Fig. 4. Firstly, the measurement probe is moved along the *y* direction until the distance between the probe and sphere along the *z*-axis are minimized. The master sphere is then moved along the *x* direction until the probe aligns as near as possible with the center position coordinate of the master sphere in the *x* and *y* directions, denoted herein as $P_s(x, y)$, where the distance between the probe and the sphere along the *z*-axis are minimized. Finally, the measurement probe is moved along a cross-shaped path on the sphere by respectively moving the probe along the *y* direction and the master sphere along the *x* direction until alignment with $P_s(x, y)$ is achieved. This operation is referred to as sphere scanning hereafter. An automatic-centering interface employing a least square method was devised to evaluate the relevant center position coordinate of the master sphere in the *x* and *y* directions, as shown in Fig. 5. $P_s(x, y)$ is obtained by fitting the measured data located in the range between cutoff lines A and B by a least square circle method. Here, $P_s(x, y)$ is taken as the position coordinate of the *c*-axis. After repeated measurement experiments, the statistical fitting results show that the calibration accuracy of the center of the master sphere is less than 1 μm.
2. The second stage involves aligning the chromatic confocal probe with the center position coordinate of the reference sphere, denoted as $P_r(x, y)$. The reference sphere scanning procedure is implemented as described above for the first stage. A 2D offset vector **Δp**, representing the relative distance between $P_s(x, y)$ and $P_r(x, y)$, is calculated as

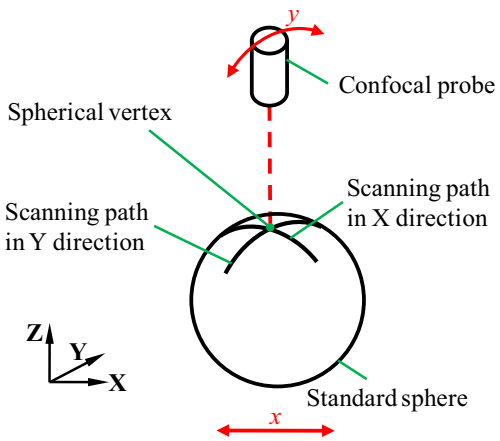

Fig. 4 Sphere scanning procedure to locate the center position of a calibration sphere

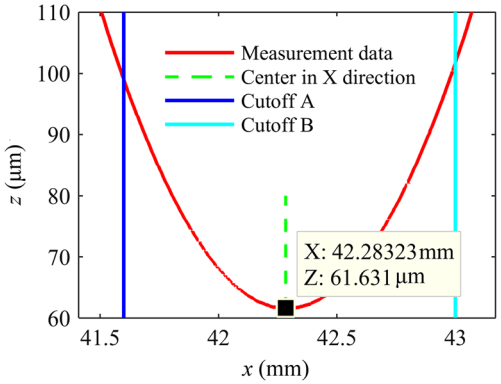

Fig. 5 Schematic of automatic-centering interface to evaluate the center position of a calibration sphere

$$\Delta \boldsymbol{p} = p_s(x,y) - p_r(x,y) \tag{2}$$

after converting $P_s(x, y)$ and $P_r(x, y)$ into vector form. The offset vector **Δp** is recorded in the control system and stored in a configuration file, completing the dual standard sphere calibration procedure for the OMM method.

The direction of the optical axis corresponds with the *z*-axis, which represents the measurement direction, and the relative distance between the master sphere and the measurement probe is adjusted by movement along the *z*-axis to ensure that the chromatic confocal sensor is in an effective measurement range; therefore, the position in the *z* direction requires no special care in the calibration process.

2.3 Measurement procedure

After calibration, the integrated reference sphere and transition arm component is disconnected from the 3R holder, and the integrated *y*-axis translation stage and chromatic confocal probe component is removed from the processing zone during workpiece machining to protect these critical components from damage due to metal fragments and coolant. After

completion of the machining process, the machined workpiece is retained on the vacuum chuck, and the OMM system components are reinstalled. Because the granite base bolted on top of the spindle ensures that the position of the System 3R holder remains absolutely stable, the reinstallation accuracy of the reference sphere is within 1 μm. Therefore, the reference sphere is able to serve as the reference orientation relative to *c*-axis and plays an essential role in guaranteeing measurement accuracy. However, the reinstalled integrated *y*-axis stage and probe component requires recalibration to ensure that its reinstalled position conforms to the previously calibrated position. Therefore, the second stage calibration discussed in the previous subsection must be repeated. It is noted that this recalibration would be required even if the component had been retained during the machining process owing to the effect of vibration on the accuracy of the installation position. This operation ensures that the optical axis of the measurement probe is aligned with the *c*-axis. The measurement procedure for different structures is described as follows.

1. For flat and spherical surfaces, the surface topography can be replaced by the topography of a 2D section profile passing through the meridian of a workpiece in general, which means that a linear scanning motion is sufficient to represent the surface topography, and this simplification is adopted in the present study. The measurement probe is moved toward the surface being measured along the negative *z* direction until reaching an appropriate position at which the distance between the probe and measured surface is located in the effective measurement range of the chromatic confocal probe. Therefore, measurements for both flat and spherical surfaces are achieved only by the linear movement of the workpiece along the *x* direction at the translational rate of 0.1 mm/s. The measurement data is recorded by the data acquisition card with a time interval of 20 ms, and an image representative of the measurement result is instantly displayed in the interface window.
2. For aspheric and non-rotationally symmetric surfaces, a 2D section profile is not sufficient to represent the actual contour of the workpiece, and 3D measurements involving the synchronous translation of the *x*-axis and rotation about the *c*-axis are required to evaluate and reconstruct the surface topography of measured workpieces. The synchronous motion of the *x*- and *c*-axes proceeds in accordance with the previous program code. The measurement probe remains fixed in the *y* direction. The measured workpiece is translated in the *x* direction while the position coordinate is measured by a linear encoder. Meanwhile, the measured workpiece rotates with respect to the *c*-axis, and the corresponding angle is recorded by a rotary encoder. The measurement data, composed of the relative distances between the measurement probe and the measured workpiece, represent a spiral curve of the machined component surface centered along the *c*-axis (as shown in Fig. 6), which are collected by the data acquisition card. A data processing program was developed to transform the data into polar form and display a 3D contour profile. This program is discussed in the following subsection.

2.4 Reconstruction of a three-dimensional surface

The parameter $P_s(x, y)$ provides the *x* coordinate of the *c*-axis, herein denoted as x_{center}, and x_{center} serves as the origin upon which the 3D surface topography of the machined component is based during the 3D reconstruction process. The discrete measurement data reflecting positions x_i obtained along the *x*-axis and angle data C_i reflecting rotation about the *c*-axis at an arbitrary point can be expressed in polar coordinates as follows.

$$\begin{cases} R_i = x_i - x_{\text{center}} \\ \theta_i = C_i \end{cases} \quad i = 1, 2, \ldots n \tag{3}$$

The precise reproduction of the 3D surface topography requires the transformation of a corresponding measurement data point from its polar coordinate representation to a Cartesian coordinate representation. The transformation process is expressed as follows.

$$\begin{cases} X_i = R_i \cos(\theta_i) \\ Y_i = R_i \sin(\theta_i) \end{cases} \tag{4}$$

The corresponding angle θ_i is recorded by a SiGNUM RESM angle encoder (Renishaw, UK) with the line count 9000 along the circumferential direction. The readhead part SR015A and interface part Si-NN-0200-20 (Renishaw, UK) are employed in the present study, and the interface part can achieve 200 subdivisions between arbitrary two adjacent lines of the angle encoder, so the angle resolution of *c*-axis is 0.72″ (0.0002°). Furthermore, the system accuracy is nominally ±3.91″ and can be improved to ±1″ after compensation by UMac, which ensures the accuracy of angle position θ_i and data processing.

Because measurements are collected at uniform time intervals, the density of the measured data points along the spiral curve decreases with increasing *R*, as illustrated in Fig. 6 for a spherical object. Therefore, the reconstruction region given by the green circle in Fig. 6 representative of the sphere's edge is divided into a uniform grid for further data processing. The grid sections near the rotational center of the measured component may contain overlapping measurement data points, which represent measurement data redundancy. Thus, the average value of overlapping data points is used to represent the final resultant data of this grid section. Using an appropriate

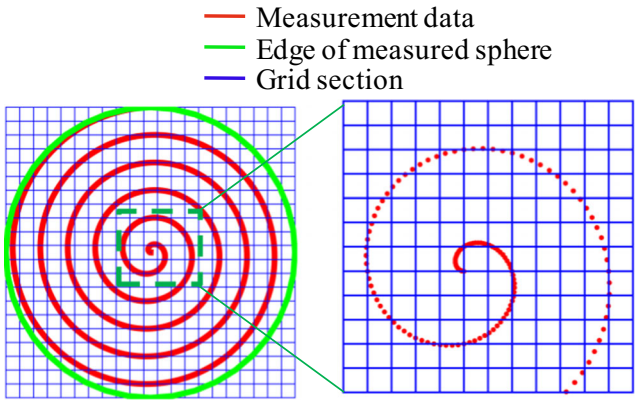

Fig. 6 Data-processing scheme for 3D reconstruction

data processing method, it is possible to show the 3D surface topography of the machined workpiece according to the coordinate data in each grid section of the reconstruction region in the designed display interface.

2.5 Experiments

To evaluate the measurement accuracy and effectiveness of the proposed OMM method, two groups of measurement experiments were conducted.

The first group involved 2D OMM. A flat surface having a 30-mm diameter was employed as a test object. In addition, a convex spherical surface was specifically designed, as shown in Fig. 7, where the diameter of the workpiece is 10 mm, the spherical radius of curvature is 150 mm, and the chord height is calculated to be approximately 83 μm, which is within the measurement range of the chromatic confocal sensor. As such, both 2D and 3D measurements are ideally suited to this spherical surface. The two workpieces were machined on a home-made ultra-precision turning machine employing a diamond tool with a nose radius of 1.038 mm. After completing the machining process, 2D OMM was conducted to extract the section profiles

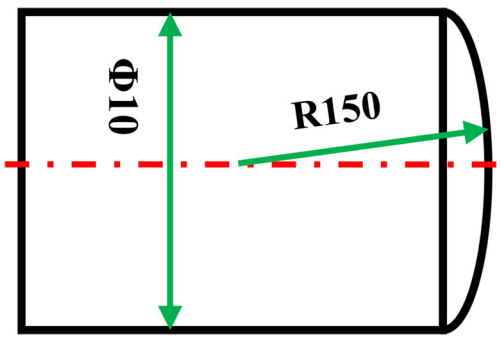

Fig. 7 Schematic diagram of the convex spherical surface employed for experimental testing

of each of the machined components. The form error can be obtained by subtracting the nominal profile from the measurement data [26]. After the machined component was measured by the proposed OMM system, it was removed from the vacuum chuck of the machining tool and measured by the Talysurf PGI 1240, and the respective measurement results compared.

The second group of measurement experiments involved the reconstruction of a 3D surface. The 3D measurement process discussed in Sect. 2.3 was conducted to evaluate and reconstruct the surface topography of the abovementioned convex spherical surface and a sinusoidal modulation structure with a 10 μm amplitude and a period of 200 μm (i.e., $y = 10\sin\left(\frac{x\pi}{100}\right)$). The sinusoidal modulation structure was measured by a WYKO NT1100 optical profiler, and the comparison is discussed in detail in Sect. 3.1.

3 Results and discussion

3.1 OMM system accuracy

For the flat surface, Fig. 8 shows a comparison of the measured data (blue curve) obtained by the proposed OMM system and the data (green curve) obtained by the Talysurf PGI 1240 system, which are appropriately scaled to make them comparable. A polynomial fitting method was employed over the radius of the workpiece from the center to 14.5 mm. The peak-valley (PV) value of the form error obtained by OMM is 0.1988 μm, while that obtained by the contact method is 0.2277 μm, and the deviation between the two

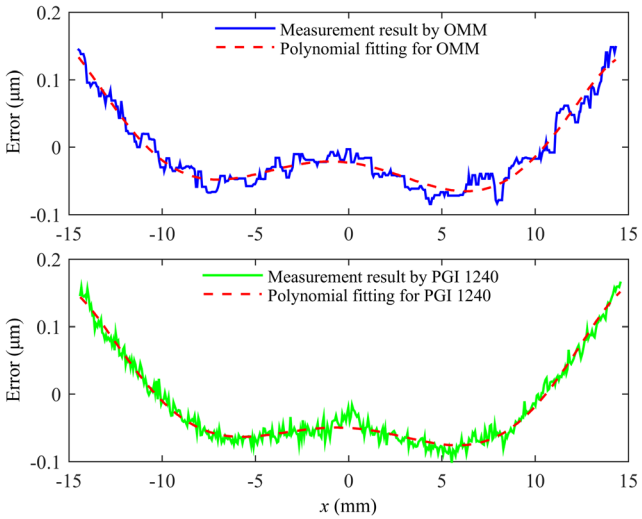

Fig. 8 Comparison of the surface measurement results for a 15-mm radius flat sample obtained by the proposed OMM system and the contact-type Talysurf PGI 1240 metrology instrument

measurement methods is 28.9 nm. As such, the measurement result obtained by OMM is very close to that provided by the contact measurement. Overall, the fitted results of the two measurement methods are essentially equivalent over the fitting range employed, and their degree of correlation is quantitatively discussed below.

For the convex spherical surface, the 2D section profile passing through the meridian of the workpiece was employed to represent the surface topography, and the form error (the deviation between the measured surface topography and the actual surface topography) is depicted in Fig. 9. The polynomial fitting results of the two measurement methods are essentially equivalent, providing an m-shape appearance, which is most likely caused by the eccentric error of the diamond tool. The degree of correlation for the two measurement methods is quantitatively discussed in the following paragraph. The PV value of the form error obtained by the OMM method was about 0.1638 μm, while that obtained by the Talysurf PGI 1240 was about 0.1187 μm, and the deviation between the two measurement methods is 45.1 nm. The fitted radius of the spherical surface obtained by OMM was approximately 148.688 mm, while that obtained by the contact method was approximately 149.114 mm, which are both less than the nominal radius of 150 mm, and a deviation between the two measurement methods of 0.426 mm is obtained. It is of note that the fitted values obtained by the proposed OMM method for the form error and the radius of the spherical surface are in all cases close to those obtained by the contact method.

Pearson's correlation coefficient was employed to describe the relationship between the measurement results obtained by OMM and the Talysurf PGI 1240 and the degree of linear dependence between the two results. Pearson's correlation coefficient is calculated as follows:

$$r_{a,b} = \frac{\sum_{i=1}^{n}\left(a_i - a\right)\left(b_i - b\right)}{\sqrt{\sum_{i=1}^{n}\left(a_i - a\right)^2}\cdot\sqrt{\sum_{i=1}^{n}\left(b_i - b\right)^2}} \tag{5}$$

where a and b represent the result datasets obtained by OMM and the contact method, respectively, n is the number of data points in a and b, and a and b are the mean values of a and b, which is calculated as follows for a, and analogously for b.

$$a = \frac{1}{n}\sum_{i=1}^{n} a_i \tag{6}$$

A complete and simplified expression of Pearson's correlation coefficient is rearranged as follows.

$$\begin{aligned} r = r_{a,b} &= \frac{n\sum_{i=1}^{n} a_i b_i - \sum_{i=1}^{n} a_i \sum_{i=1}^{n} b_i}{\sqrt{n\sum_{i=1}^{n} a_i^2 - \left(\sum_{i=1}^{n} a_i\right)^2}\cdot\sqrt{n\sum_{i=1}^{n} b_i^2 - \left(\sum_{i=1}^{n} b_i\right)^2}} \\ &= \frac{\sum_{i=1}^{n} a_i b_i - na\cdot b}{\sqrt{\left(\sum_{i=1}^{n} a_i^2 - na^2\right)}\cdot\sqrt{\left(\sum_{i=1}^{n} b_i^2 - nb^2\right)}} \end{aligned} \tag{7}$$

According to the Eqs. (5)–(7), $r = 0.958$, the coefficient of determination r^2 is 0.918 in the fitting range employed for the flat surface. For the convex spherical surface, $r = 0.770$ and $r^2 = 0.593$. The statistical data indicates that the measurement results obtained by the proposed OMM system and the Talysurf PGI 1240 system are strongly correlated for both the flat and convex spherical surfaces.

Comparisons of the measurement results given in Figs. 8 and 9, and the statistical data indicate that the systematic accuracy of the proposed OMM system is at an equivalent level as the Talysurf PGI 1240 metrology instrument, which leads to the conclusion that the proposed OMM system is feasible for accurately measuring high precision 2D surfaces and is similarly effective for evaluating the form error as the contact method. The observed deviations between the measurement data obtained by the two methods are within an acceptable range.

3D measurements were conducted to show the 3D contoured topography of the machined convex spherical surface and the sinusoidal modulation structured surface. The measurement processes for the spherical and sinusoidal modulation surfaces respectively employed x-axis displacements of 5 and 2.5 mm, and a c-axis rotation of 3600° over a measurement period of 30 s with a sampling interval of 100 ms. The collected measurement data was subjected to the data processing presented in Sect. 2.4 to reconstruct the data.

Figure 10 shows the 3D topography of the convex spherical surface, which is consistent with the structure of the

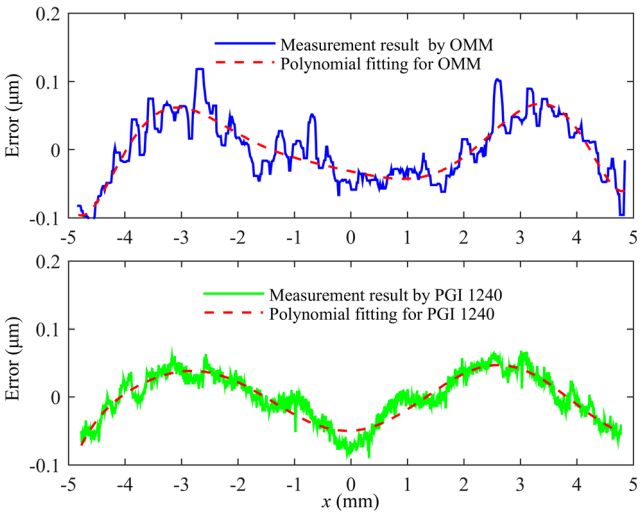

Fig. 9 Comparison of the surface measurement results for the 5-mm radius convex spherical surface given in Fig. 7 by the OMM system and the Talysurf PGI 1240

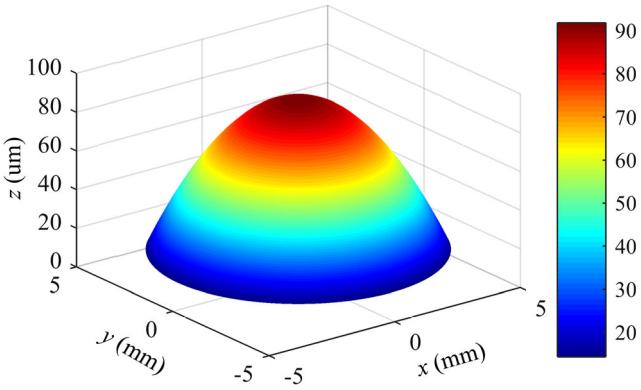

Fig. 10 The 3D topography of the convex spherical surface given in Fig. 7 based upon measurements obtained by the OMM system

machined component in Fig. 7. Figures 11 and 12 illustrate the surface topography of the sinusoidal structure, as measured by the WYKO NT1100 optical profiler and the proposed OMM system, respectively. Surface topography was measured by the optical profiler within an effective view field of 0.9 mm × 1.2 mm along the radius of the component, and the corresponding 2D section profile was extracted, as shown in Fig. 11, where the amplitude is about 9.8 μm and period is approximately 199.33 μm. The entire sinusoidal surface was measured by OMM to reveal the overall 3D surface topography, and a 2D section profile passing through the meridian was extracted to reveal the surface topography and form error, as depicted in Fig. 12, where the amplitude is measured to be about 10.037 μm and the period approximately 200 μm, which are in very good agreement with the optical profiler results. The observed consistency with the optical profiler results indicates that the proposed OMM method is effective for evaluating 3D surface topography. Comparison of the 2D section profiles shown in Figs. 11 and 12 demonstrates some differences between the two waveforms, where the waveform in Fig. 12 is rough and contains some data distortion relative to the waveform in Fig. 11. These differences may be caused by a sampling interval that is overly large relative to the translation rate in the *x* direction and rotation rate about the *c*-axis, resulting in a sparsity of sampling data.

3.2 Uncertainty analysis

The ultra-precision machining tool is operated inside a clean room, where the temperature and relative humidity are controlled, respectively, to 20 ± 0.5 °C and 50 ± 3 %. To ensure better OMM system stability, the ultra-precision machining tool is operated in conjunction with a vibration isolation system [27] having advanced vibration isolation features to eliminate low frequency vibrations greater than 3 Hz. As such, the effect of temperature, humidity, and vibration on the measurement uncertainty is neglected in the uncertainty analysis. Besides, reinstallation accuracy of the reference sphere is a factor to be considered in the uncertainty analysis. The reinstallation accuracy is within 1 μm and ultimately causes the misalignment error between the optical axis of measurement probe and the actual the rotary axis of *c*-axis. The misalignment error will contribute to greater influence on the measurement result of spherical surface than that of flat surface, so we take the spherical surface (shown in Fig. 7) as an example to explain the influence of misalignment error on the measurement result; the numerical simulation results show that the misalignment error of 1 μm along radial direction leads to the maximal measurement deviation of 8.9 nm for the spherical surface, which is less than the resolution of the measurement probe and does not seriously affect the measurement accuracy of proposed method; therefore, the influence of reinstallation accuracy of the reference sphere is ignored in the uncertainty analysis.

The three primary factors contributing to the uncertainty are the resolution of the measurement probe, system noise, and the lateral straightness (flatness) of the *x*-axis hydrostatic slideway.

The linear resolution of the chromatic confocal measurement probe is 12 nm according to its user manual. System noise testing was performed by holding the measurement probe perpendicular to the measured surface with the *x*-, *y*-, and *z*-axis positions held fixed and collecting position measurements using a time increment mode with a time interval of 20 ms over a total measurement time of about 140 s. The

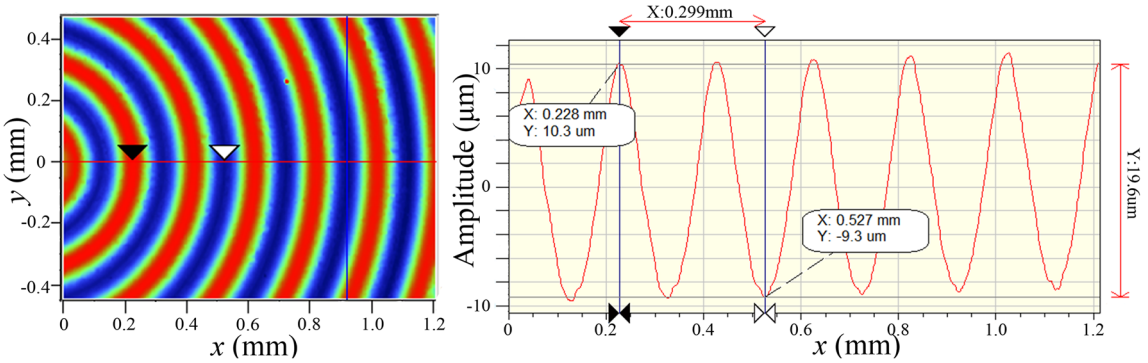

Fig. 11 The surface topography of the sinusoidal modulation structure obtained by a WYKO NT1100 optical profilometer scanned along the machined component radius

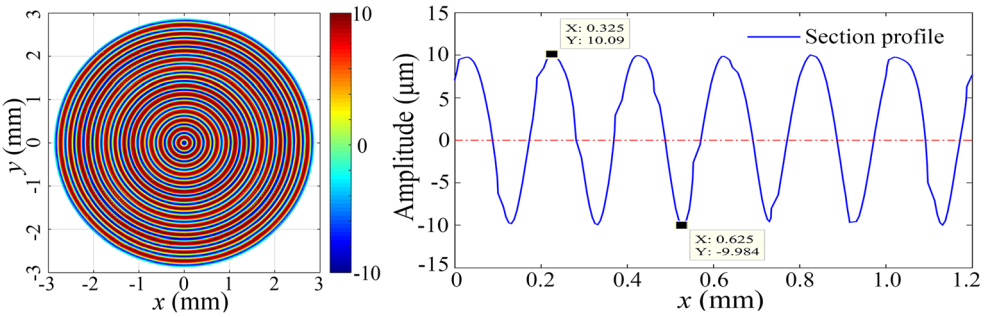

Fig. 12 The surface topography of the sinusoidal modulation structure obtained by the OMM system

system noise generated by the data acquisition card is around 20 nm. The flatness uncertainty of the *x*-axis slideway is mainly determined by the manufacturing accuracy, assembly accuracy, and the long-term dimensional stability of its structure. Translation along this sensitive direction seriously affects the measurement accuracy. The lateral straightness was calculated by a photoelectric autocollimator (CCD-AI, Jiujiang Haibo Technology Co Ltd., China) to be 80 nm along the entire 160-mm displacement path. The uncertainty analysis of the OMM system was conducted using the analysis approach described in the literature [28], which provides a combined standard uncertainty value. This value for the OMM system presented in the current study is 83.33 nm, which mainly arises from uncertainty in the flatness of the *x*-axis slideway.

4 Conclusions

The present work integrated a chromatic confocal measurement system with a home-made ultra-precision diamond turning machine to achieve the non-contact OMM of machined components. The following presents the main procedures discussed and the conclusions obtained based on the results of experimental testing.

1. Two standard spheres were carefully selected to determine the position of the rotary axis of the spindle according to a sphere scanning procedure described in detail. The calibration method can establish the position of the rotary axis with an accuracy of 1 μm.
2. The measurement probe obtained excellent linear measurement accuracy performance, and an *RME* of 0.022 % was obtained. The experimental results demonstrated that the measured values obtained by the proposed OMM system were very close to the values provided by the contact-type Talysurf PGI 1240 metrology instrument for 2D measurements, and the systematic accuracy of the OMM system was shown to represent an equivalent level as that of the Talysurf PGI 1240. In addition, the presented OMM method was shown to be capable of reconstructing the 3D surface topography of flat, spherical, and aspheric surfaces. Integrating the OMM system with an ultra-precision machining tool enables the tool to realize the function of processing-measurement integration.
3. To estimate the overall measurement uncertainty, several sources of error were considered: the resolution of the chromatic confocal probe, system noise caused by the control system, and the lateral straightness along the *x*-axis. The combined standard uncertainty of the proposed OMM system was estimated to be 83.33 nm, which mainly arose from the flatness uncertainty of the *x*-axis hydrostatic slideway.

Acknowledgments The present work was supported by the NSAF (Grant No. U1530106) and the National Natural Science Foundation of China (Grant No. 51005061). We thank LetPub (www.letpub.com) for its linguistic assistance during the preparation of this manuscript.

References

1. Vacharanukul K, Mekid S (2005) In-process dimensional inspection sensors. Measurement 38:204–218. doi:10.1016/j.measurement.2005.07.009
2. Liu ZQ (1999) Repetitive measurement and compensation to improve workpiece machining accuracy. Int J Adv Manuf Tech 15:85–89. doi:10.1007/s001700050043
3. Shiraishi M (1989) Scope of in-process measurement, monitoring and control techniques in machining processes—part 2: in-process techniques for workpieces. Precis Eng 11:27–37. doi:10.1016/0141-6359(89)90006-8
4. Yandayan T, Burdekin M (1997) In-process dimensional measurement and control of workpiece accuracy. Int J Mach Tool Manu 37:1423–1439. doi:10.1016/S0890-6955(97)00019-9
5. Huang H, Lei XY, Wang J, Xu Q, He LY, Guo YB (2010) A machining error compensation method using on-machine profile measurement in 3-axis aspheric grinding. Adv Mat Res 154-155:390–395. doi:10.4028/www.scientific.net/AMR.154-155.390
6. Kim H, Lee K, Lee K, Bang Y (2009) Fabrication of free-form surfaces using a long-stroke fast tool servo and corrective figuring with on-machine measurement. Int J Mach Tool Manu 49:991–997. doi:10.1016/j.ijmachtools.2009.06.011
7. Chen FJ, Yin SH, Huang H, Ohmori H, Wang Y, Fan YF, Zhu YJ (2010) Profile error compensation in ultra-precision grinding of aspheric surfaces with on-machine measurement. Int J Mach Tool Manu 50:480–486. doi:10.1016/j.ijmachtools.2010.01.001
8. Rahman MS, Saleh T, Lim HS, Son SM, Rahman M (2008) Development of an on-machine profile measurement system in ELID grinding for machining aspheric surface with software

compensation. Int J Mach Tool Manu 48:887–895. doi:10.1016/j.ijmachtools.2007.11.005
9. Liu HB, Wang YQ, Jia ZY, Guo DM (2015) Integration strategy of on-machine measurement (OMM) and numerical control (NC) machining for the large thin-walled parts with surface correlative constraint. Int J Adv Manuf Technol 80:1721–1731. doi:10.1007/s00170-015-7046-x
10. Huang ND, Zhang SK, Bi QZ, Wang YH (2016) Identification of geometric errors of rotary axes on 5-axis machine tools by on-machine measurement. Int J Adv Manuf Technol 84:505–512. doi:10.1007/s00170-015-7713-y
11. Zhang GY, Xu XP, Fu XH, Yang L, Li CZ (2002) The measurement and control of diameter in large-scale part processing. J Mater Process Tech 129:653–657. doi:10.1016/S0924-0136(02)00675-1
12. Yan T, Su XY, Liu YK, Jing HL (2008) 3D shape measurement of the aspheric mirror by advanced phase measuring deflectometry. Opt Express 16:15090–15096. doi:10.1364/OE.16.015090
13. Fan KC, Chao YH (1991) In-process dimensional control of the workpiece during turning. Precis Eng 13:27–32. doi:10.1016/0141-6359(91)90218-8
14. Gao Y, Huang X, Zhang Y (2010) An in-process form error measurement system for precision machining. Meas Sci Technol 21:54001–54008. doi:10.1088/0957-0233/21/5/054001
15. Sasaki O, Hashimoto K, Fujimori Y, Suzuki T (2001) Measurement of cylinder diameter by using sinusoidally vibrating sinusoidal gratings. Proc SPIE 4416:35–38. doi:10.1117/12.427062
16. Tomlinson R, Coupland JM, Petzing J (2003) Synthetic aperture interferometry: in-process measurement of aspheric optics. Appl Opt 42:701–707. doi:10.1364/AO.42.000701
17. Shiraishi M, Yasui A (1998) In-process measurement of dimensional error for stepped workpiece profile. J Manuf Sci Eng 120:202–206. doi:10.1115/1.2830104
18. Kohno T, Matsumoto D, Yazawa T, Uda Y (2000) Radial shearing interferometer for in-process measurement of diamond turning. Opt Eng 39:2696–2699. doi:10.1117/1.1290463
19. Ko TJ, Park JW, Kim HS, Sun HK (2007) On-machine measurement using a noncontact sensor based on a CAD model. Int J Adv Manuf Tech 32:739–746. doi:10.1007/s00170-005-0383-4
20. Zhu YJ, Na JX, Pan WQ, Zhi YN (2013) Discussions on on-machine measurement of aspheric lens-mold surface. Optik-International Journal for Light and Electron Optics 124:4406–4411. doi:10.1016/j.ijleo.2013.01.106
21. Luo D, Kuang C, Liu X (2012) Fiber-based chromatic confocal microscope with Gaussian fitting method. Opt Laser Technol 44:788–793. doi:10.1016/j.optlastec.2011.10.027
22. Quinsat Y, Tournier C (2012) In situ non-contact measurements of surface roughness. Precis Eng 36:97–103. doi:10.1016/j.precisioneng.2011.07.011
23. Minoni U, Manili G, Bettoni S, Varrenti E, Modotto D, De Angelis C (2013) Chromatic confocal setup for displacement measurement using a supercontinuum light source. Opt Laser Technol 49:91–94. doi:10.1016/j.optlastec.2012.11.006
24. Nouira H, El-Hayek N, Yuan X, Anwer N (2014) Characterization of the main error sources of chromatic confocal probes for dimensional measurement. Meas Sci Technol 25:44011. doi:10.1088/0957-0233/25/4/044011
25. Rishikesan V, Samuel GL (2014) Evaluation of surface profile parameters of a machined surface using confocal displacement sensor. Procedia Materials Science 5:1385–1391. doi:10.1016/j.mspro.2014.07.456
26. International Organization For Standardization (2010) ISO 25178 Geometrical product specification(GPS)-surface texture: Areal-Part 602. Nominal characteristics of non-contact (chromatic confocal probe) instruments. 2010
27. Zou XC, Li ZQ, Zhao XS, Sun T, Zhang KP (2014) Study on the auto-leveling adjustment vibration isolation system for the ultra-precision machine tool. Proc SPIE-The International Society for Optical Engineering 9281(2):S108. doi:10.1117/12.2069463
28. JCGM (2008) Evaluation of measurement data-guide to the expression of uncertainty in measurement. 2008